# Modeling of Turbulent Separation Flow

**Dr. Imad Shukry Ali** **Sahab Shehab Ahmed***
**College of Eng./Mech, Eng.Dept**
**Babylon University- / Iraq.**
**Emad.Ali6@gmail.com** **sihebshehab_1985@yahoo.com**

**ABSTRACT**

In the present work a numerical analysis includes modeling of separation flow of a two-dimensional, incompressible, steady and turbulent flow around (NACA 0012) airfoil. The study includes the numerical solution of the continuity and momentum equations with the two equations of the ($k$-$\varepsilon$) turbulence model. Grid generation with Body Fitted Coordinates System (BFCS) has been used. The grid generation technique based on differential equations which it solve by finite difference method and the clustering of the grid was used in the numerical solution. The Finite Volume Method (FVM) is adapted to solve Navier-Stokes equation by transferring these equations from differential forms to algebraic forms which can be solved according to the (SIMPLE algorithm) procedure with collocated grid arrangement The flow variables (aerodynamic characteristics) such as the velocity vector and stream function are computed. Beside, pressure, lift and drag coefficients. The present study gives a detail description of separation flow and its effects under different flow conditions. Separation point at the airfoil surface is predicted at high angles of attack. It is found that increase the angle of attack will lead to increases all of separation occurrence, recirculation, reversed flow also, pressure, lift and drag coefficients are highly influenced by the angle of attack and the Reynolds number before stall angle.

The numerical results were compared with other pervious experimental and theoretical results. The agreement was good, confirming the reliability of the proposed computational algorithm in calculating the turbulent separation flow around (NACA 0012) airfoil.

**Keywords**: Separation , CFD , Turbulent flow , NACA 0012.

## NOMENCLATURE:

| Symbol | quantity | unit |
|---|---|---|
| $a_1$, $a_2$ | Transformation coefficients | |
| $C_p$ | Pressure coefficient | |
| $p$ | Pressure, | $(N/m^2)$ |
| $Q$ | Control function | |
| $Re$ | Reynolds number | |
| $S_N$ | Source term due to non orthogonal characteristic of grid system | |
| $S_\phi$ | Linearized source term for $\phi$ | |
| $G_1$ | Contravariant velocity component in x-direction, | (m/s) |
| $u$ | Velocity component in x-direction, | (m/s) |
| $G_2$ | Contravariant velocity component in y-direction, | (m/s) |
| $v$ | Velocity component in y-direction, | (m/s) |
| $x$ | Cartesian coordinate in horizontal direction, | (m) |
| $Y$ | Dimensionless Coordinate in vertical direction | |
| $y$ | Cartesian coordinate in vertical direction, | (m) |
| $\theta$ | Dimensionless temperature | |
| $\phi$ | Variable vector | |
| $\Gamma_\phi$ | Diffusion coefficient | |
| $v$ | Kinematic viscosity of the fluid, | $(m^2/s)$ |
| $\rho$ | Density of the fluid, | $(kg/m^3)$ |
| $\xi$, $\eta$ | Dimensionless body-fitted coordinates | …… |

## 1. INTRODUCTION

Flow separation is a natural phenomenon as well as an engineering problem of fundamental importance in numerous aerodynamics applications including flows over aircrafts, wings/airfoils, cylinders and turbine blades. Airfoil moving through a fluid cause flow separation. In this case, the turbulence that is generated behind the airfoil is called a wake. Very turbulent wakes occur behind moving airfoil in air. The effect of the turbulent wake is to lower the settling velocity of the particles, because a part of the fluid movement in the eddy is against the direction of movement of the particles, and exerts a drag force on the particles. It spoils the performance of the airfoil. **Chris at el [1]** investigated the aerodynamic characteristics of the NACA 0012 airfoil section at range of angle of attack from zero to 180 deg. Data were obtained at a Reynolds number $1.8 \times 10^6$ with airfoil surface smooth. **Cerfacs[2]** calculated the flow around low speed, high lift two dimensional airfoil ($Re=2.1 \times 10^6$ , $M=0.15$ ) with the object to be able to predict stall. Had been carried out improving the numerical scheme, as well as implementing and testing different turbulent model, such as the Baldwin- Lomax model, various (k-ε) model . **Cerfacs[3]** studied the flow around low speed high lift two dimensional airfoil with the object to be able to

predicted stall. The flow condition of the case were ($Re=2.1x10^6$ , M =0.15 ) and angle of attack from zero to 19 deg. **Davidson[4]** used a second moment Reynolds Stress Transport Model (RSTM) for computing the flow around a two dimensional airfoil. An incompressible SIMPLE code was used, employing a non- staggered grid arrangement. **Reece E. Neel[5]** studied and discussed numerical algorithm for turbulent flow with separated flow for two cases, converging diverging duct and flow around airfoil. **Yoshinodai at al[6]** investigated a flow around subsonic airfoil. Two and three dimension incompressible Navier stokes equation were solved by finite difference approximation without using any turbulence models. **Dahlstrom and Davidsony[7]** used Large Eddy Simulation (LES) to calculate the flow around the Aerospatiale A-profile airfoil at an angle of attack of 13.3 degree at Reynolds number of 2.1 $x10^6$. The method used was an incompressible implicit second-order finite volume method with a collocated grid arrangement. **Dahlstrom and Davidson [8]** presented Large Eddy Simulation (LES) of flows around simple, two-dimensional airfoils . The specific case chosen was the subsonic flow around the Aerospatiale A-profile at an incidence of $\alpha$=13.3degree at Reynolds number of $2.1x10^6$.The method used an incompressible implicit second-order finite volume method with a collocated grid arrangement. **Dahlstrom and Davidson[9]** studied the subsonic flow around the Aerospatiale A-profile at an incidence of 13.3 degree at Reynolds number of $2x10^6$ was using Large Eddy Simulation (LES). **Kawai and Fuji[10]** investigated prediction of stall phenomenon of NACA64A006 airfoil numerically using Large Eddy Simulation (LES)/ Reynolds-Averaged Navier-Stokes (RANS) hybrid methodology with high order compact differencing scheme. Subsonic flow of $M\infty = 0.17$ with the high Reynolds number of $Re = 5.8x10^6$ was considered and the angle of attack was varied from 4.0 through 11.0deg. **Rupesh at al[11]** developed predictions of the flow around the Aerospatiale-A airfoil at maximum lift, $\alpha$= 13.3 deg, and Re = $2x10^6$ were using solutions of the steady Reynolds-averaged Navier-Stokes (RANS) equations and using Detached-Eddy Simulation. **Kurzin [12]** investigated a model for separated incompressible flow past thin airfoils in the neighborhood of the "shock less entrance" condition was constructed based on the averaging of the vortex shedding flow past the airfoil edges. **Eisenbach** and **Friedrich [13]** studied incompressible flow separating from the upper surface of an airfoil at an 18° angle of attack and a Reynolds number of $Re = 10^5$, based on the free stream velocity and chord length $c$, was studied by the means of large-eddy simulation (LES).

## 2. Physics of Separated Flows

Regions of separated flow are common in many engineering applications. Separation is the entire process in which the boundary layer flow breaks down and departs from the wall surface. This physical phenomena can have a large impact on the performance of any design. It is often possible to avoid separation by placing limitations on the operating conditions, but there are times when separated flow cannot be avoided and must therefore be dealt with. In these situations it is important to know and understand the effects of separation on a particular design

Separation is the term used to describe the entire process in which a flow detaches from a solid surface, causing a breakdown of the boundary layer. When this process occurs, the boundary layer undergoes a sudden thickening, causing an increased interaction between the viscous-in viscid layers. When separation

occurs on smooth surfaces such as airfoils and flat plates, it is usually the result of an adverse pressure gradient. As the pressure increases along the primary flow direction, the flow velocity responds by decelerating. If this pressure differential continues, the flow velocity will eventually come to zero and a reversal of the flow will occur. Whether the flow field is considered steady or unsteady, the location at which flow reversal occurs will vary along the wall **[5].**

The numerical computations involving turbulence modeling focus on flows with adverse pressure gradients and boundary layer separation. It may therefore be insightful to

discuss some of the understanding of turbulent flow separation.

### 3. PROBLEM DESCRIPTION AND THE MATHEMATICAL MODEL

The present model consists of a two-dimensional inclined turbulent separation flow around airfoil (NACA 0012)

The numerical solution is obtained by using a finite volume scheme and the following assumptions are considered in the present analysis :

1. The fluid flow is steady.
2. The fluid flow is incompressible.
3. The fluid flow is fully viscous.
4. The fluid flow is subsonic.
5. The turbulence is isotropic.
6. Fluid flow is Newtonian and
7. The fluid flow is two-dimensional.

The turbulent external two-dimensional flow distribution around airfoil is described by the Navier–Stokes equations. The governing equations are transformed into a dimensionless forms by using the following dimensionless variables **[12]**:-

continuity equation

$$\frac{\partial u}{\partial x}+\frac{\partial v}{\partial y}=0 \qquad (1)$$

X-Direction ($u$-momentum)

$$\rho\left(u\frac{\partial u}{\partial x}+v\frac{\partial u}{\partial y}\right)=-\frac{\partial P}{\partial x}+\frac{\partial}{\partial x}\left(2\mu_{eff}\frac{\partial u}{\partial x}\right)+\frac{\partial}{\partial y}\left(\mu_{eff}\frac{\partial u}{\partial y}\right)+\frac{\partial}{\partial y}\left(\mu_{eff}\frac{\partial v}{\partial x}\right) \qquad (2)$$

Y-Direction ($v$-momentum)

$$\rho\left(u\frac{\partial v}{\partial x}+v\frac{\partial v}{\partial y}\right)=-\frac{\partial P}{\partial y}+\frac{\partial}{\partial x}\left(\mu_{eff}\frac{\partial v}{\partial x}\right)+\frac{\partial}{\partial y}\left(2\mu_{eff}\frac{\partial v}{\partial y}\right)+\frac{\partial}{\partial x}\left(\mu_{eff}\frac{\partial u}{\partial y}\right) \qquad (3)$$

a) X: Momentum

$$\frac{\partial}{\partial\xi}(\rho G_1 u)+\frac{\partial}{\partial\eta}(\rho G_2 u)=\frac{\partial}{\partial\xi}\left(\Gamma_u Ja_1\frac{\partial u}{\partial\xi}\right)+\frac{\partial}{\partial\eta}\left(\Gamma_u Ja_2\frac{\partial u}{\partial\eta}\right)+S_{MX}$$

Y: Momentum

$$\frac{\partial}{\partial\xi}(\rho G_1 v)+\frac{\partial}{\partial\eta}(\rho G_2 v)=\frac{\partial}{\partial\xi}\left(\Gamma_v Ja_1\frac{\partial v}{\partial\xi}\right)+\frac{\partial}{\partial\eta}\left(\Gamma_v Ja_2\frac{\partial v}{\partial\eta}\right)+S_{MY}$$

*k*- Equation

$$\frac{\partial}{\partial\xi}(\rho G_1 k)+\frac{\partial}{\partial\eta}(\rho G_2 k)=\frac{\partial}{\partial\xi}\left(\Gamma_k Ja_1\frac{\partial k}{\partial\xi}\right)+\frac{\partial}{\partial\eta}\left(\Gamma_k Ja_2\frac{\partial k}{\partial\eta}\right)+S_k$$

ε- Equation

$$\frac{\partial}{\partial\xi}(\rho G_1 \varepsilon)+\frac{\partial}{\partial\eta}(\rho G_2 \varepsilon)=\frac{\partial}{\partial\xi}\left(\Gamma_\varepsilon Ja_1\frac{\partial \varepsilon}{\partial\xi}\right)+\frac{\partial}{\partial\eta}\left(\Gamma_\varepsilon Ja_2\frac{\partial \varepsilon}{\partial\eta}\right)+S_\varepsilon$$

## 3. BOUNDARY CONDITIONS

The boundary conditions as shown in figure (1) which are used in the present study can be arranged as follows:-

**1.**At inlet the velocity component (u , v ) ,the static pressure ,the turbulent kinetic energy k and its dissipation rate ε are specified as shown in figure()

2. When C-type grid is used, there will be a branch cut across the wake region to maintain a simple connected region. Since physically the flow variables are continuous across this cut, the fluid properties in this cut are specified as averages of the variable one point above and one point below the cut line.

3. The boundary conditions that are imposed upon the body surface are the usual impermeability and no-slip condition all time **[43].** In the present case, the value of all variables are chosen equal to zero.

4. The boundary of far field conditions (the region which it properties equal to free stream condition). This led to the normal gradient of all dependent variables to be zero.

5. Always, all values of dependent variables are unknown at exit boundary. It is often adequate to set outlet boundary values equal to intermediate up stream neighbor.

## 4. NUMERICAL SCHEME

The grid generation calculation is based on the curvilinear coordinate system applied to fluid flow as described by **Thompson et al. [13]**. **Fig.(2)** shows the schematic of two dimensions body fitting grid used for the present computation. This grid is obtained by solving non-homogeneous 2-D Poisson equations [14]:-

.

## 5. RESULTS AND DISCUSSION

This section will describe the various results of subsonic aerodynamics of airfoil obtained in this paper, also include the discussion of these results. In order to verify the numerical results that are obtained in the present study which computational program and mathematical model developed in this study are correct, it is necessary to compare these results with the results from previous work. The fluid flow separation field distribution around NACA 0012 airfoil is compared with computational work by **[50]** at Reynolds number ($10^6$) and angle of attack (20 degree). Good agreement has been obtained as show in figure (4). When a turbulent boundary really starts to swirl, the boundary layer thickness starts to grow even faster. Eventually, the flow is so mixed, it starts to flow back towards the front of the surface. When this happens, the outside, original fluid is moving over a large bubble created by the turbulence. Inside the bubble, the flow is moving back up the surface. This is called flow separation. The front of the bubble, where the outside fluid turns sharply away from the surface, is called the point of separation, the back of the bubble, where the outside fluid turns back to follow the surface again, is called the point of reattachment. If the region of flow separation extends past the surface, this region is called a wake. Stream line distribution and Velocity vectors around the airfoil (NACA0012) at angles of attack (14 and 20) degrees respectively, with two value of Reynolds number ($1.5x10^6$ and $2.5x10^6$) based on chord . It is so clear that the velocity vectors at a low angle of attack are not effected by increase the velocity, the flow is attached to the airfoil boundary and the working area is increased to increase the lift as a result. It is ensured the separation zone approximately is bit. At the post stalled region at angle≈14 degree, a reversed flow is growing and moving upstream at the upper surface of the airfoil which represents the separated flow region to reach approximately 70% of the chord. At increase angle of attack (at 20 degree) the separation point is shifted toward the leading edge, the separated flow region to reach approximately (85-90)% of the chord.

The pressure distribution around the airfoil is an important parameter, both in terms of aerodynamic characteristics (because it determines the lift and drag coefficients of the airfoil) and in terms of boundary-layer behavior (because the pressure gradient is known to affect the development of turbulent boundary layers). Figures (7,8,9and10) present pressure coefficient curves for the upper ($C_{pU}$) and lower ($C_{pL}$) of the airfoil, plotted against the percent chord ($x/c$) for fluid flow around the (NACA 0012) airfoil as the angle of attack range (0,5,10,12,14,16,18 and 20)degrees with Reynolds numbers ($1x10^6$, $1.5x10^6$, $2x10^6$and $2.5x10^6$) respectively. Figure (7) shows the pressure coefficient plots for a Reynolds number of Re=$1x10^6$, to summarize the effect of variation of α on $C_p$ distribution curves, the surface pressure distribution on the lower surface of the airfoil does notably change with the increasing angle of attack up to≈14 deg, the surface pressure distribution on the upper surface of the airfoil was found to significantly vary at different angles of attack. As the angle of attack was relatively small i.e.,≥AOA degree, the surface pressure coefficient profiles along the airfoil upper surface were found to rapidly reach their negative peaks at locations quite near to the airfoil leading edge, then the surface pressure gradually and smoothly recovered over the upper surface of the airfoil up to the airfoil trailing edge. The plateau region is

absent for α=0, but a clearly developed plateau can be seen for $\alpha \geq 14°$ which it approximate at X/C=0.4.
The effect of variation of α on $C_p$ distribution curves, it can be observed in these figures that the upper surface pressure coefficients drastically change to higher negative values with increasing angle of attack up to stall angle ($\alpha \approx 14°$) after this angle, the upper surface pressure coefficients drop to lower values. The wing tip vortices become stronger with increase in angle of attack and the flow is further energized. This leads to lower pressures at the airfoil tips and the resultant drop in pressure coefficients**.** Also, Computations at various angles of attack in this range show that the separation bubble gradually develops with increase in the angle of attack**.** Notice that as Reynolds numbers increases, the upper and lower surface pressure coefficients are decreased. The increase in pressure behind the separation bubble has a reversed trend with the pressure increase being inversely proportional to Reynolds number.

The lift and drag coefficients of the airfoil at different angle of attack and Reynolds number were determined by numerically integrating the pressure distribution around the airfoil, and the results are shown in Figures (11) and (12) respectively. As the angle of attack is relatively small (i.e.,< 10 degree), the adverse pressure gradient over the upper surface of the airfoil is mild. As revealed from the pressure coefficient distributions results given above, the turbulent boundary layer around the airfoil would attach to the airfoil surface faithfully all the way from the leading edge to the airfoil trailing edge, and no flow separation was found. Therefore, the drag coefficient of the airfoil was very small and nearly a constant at different angel of attack. The lift coefficient of the airfoil was found to increase almost linearly with the increasing angle of attack. The adverse pressure gradient on the upper surface of the airfoil would become more severe as the angle of attack increasing. Since the turbulent boundary layer is unable to withstand any significant adverse pressure gradient, it would separate from the upper surface of the airfoil, and turbulent flow separation would occur as the angle of attack becoming bigger than 10 degrees. The flow separation is evident as the “plateau” region in the calculation surface pressure coefficient profiles. The separated turbulent boundary layer would generate vortex structures, and the turbulent flow could reattach to the upper surface of the airfoil as a turbulent boundary by forming a separation bubble on the airfoil. Since the reattached turbulent boundary could attach to the upper surface of the airfoil firmly from the reattachment point up to the airfoil trailing edge, the lift coefficient of the airfoil was found to keep on increasing with the increasing angle of attack. However, the increase rate was found to slow down due to the formation of the separation bubble. The drag coefficient of the airfoil was also found to increase slightly with the increasing angle of attack. As the angle of attack reaches 12 degrees, the adverse gradient becoming so severe that the separation bubble burst suddenly, and the separated boundary layer could not reattach to the upper surface of the airfoil anymore. Large-scale flow separation was found to occur over entire upper surface of the airfoil as visualized in the calculations given above, and the airfoil was found to stall completely. Therefore, the lift coefficient was found to drop rapidly, and the drag coefficient increased significantly. After airfoil stalls, the lift coefficient of the airfoil was found to increase slowly, and the drag coefficient increases rapidly with the increasing angle of attack.
Figure (13) shows the relation between the drag coefficient and the lift coefficient at difference Reynolds number. It can be seen from figure (11) that the lift coefficient increase with increase Reynolds number pending stall angle occur after this angle the lift coefficient decrease while, drag coefficient decreases with the increase of Reynolds number until stall angle, after stall angle drag coefficient decreases with the increase of Reynolds number down due to the formation of the separation bubble and large of circulation. At angle (≈14˚), the flow separates over the entire surface and full stall occurs. At this point, the lift force is markedly reduced while the drag force is drastically increased. This causes a typical aircraft to rapidly lose altitude, with partial loss of maneuverability from the airfoil, and a tendency to spin.

## 6. CONCLUSIONS

The computations were performed for different Reynolds numbers and different angles of attack. Importance conclusions from this study as follows:

**1.** The results show that the present numerical method is accurate and the extension of the SIMPLE algorithm is applicable. It is noticed from turbulence models that the ($k$-$\varepsilon$) model gives good prediction for flow separation around (NACA0012) airfoil.

**2.** Maximum lift coefficient obtained in the present study about ($C_L \approx 1.45$) at angle of attack ≈13 degree and Reynolds number $2.5 \times 10^6$.

**3.** Stall angle of (NACA0012)airfoil occurs at angle of attack ≈14.5 degree.
which agrees with experimental work by **[1]**.

4.The lift coefficient increases with increase of Reynolds number until the stalling angle occurs.

**5.**fine grid generation(C-Type grid generation) gives accurate solution with finite volume method.

**6.** The comparison between prediction and previous experimental work shows the turbulence model and numerical method employed in present work which are precise and reliable.

## REFERENCES

**[1]-** Chris, C., Critzos, Harry, H. ,Heyson, and Robert, W. " Aerodynamic Characteristics of The NACA 0012 Airfoil Section" National Advisory Committee For Aeronautics, 1955.

**[2]**- Greory , N. and O'reilly, C. L. "Low-Speed Aerodynamic Characteristics of NACA 0012 Aerofoil Section, including the Effects of Upper-Surface Roughness Simulating Hoar Frost" London , Her Majesty's Stationery Office, 1973.

**[3]**- Davidson, L. Cerfacs "Predicting Stall of a two – dimensional Airfoil Using an Algebraic Reynolds Stress Model"42, AV. Gustave Coriolis 31057 Toulouse, France, Report TR/RE/91/52, 1991

**[4]**- Davidson, L. Cerfacs "calculation of the Flow around A-Airfoils Using An Incompressible Code Based on SIMPLE and Two Layer k-ε model " 42, AV. Gustave Coriolis 31057 Toulouse, France, Report TR/RE/92/73, 1991.

**[5]-** Neel. R. E , "Advances In Computational Fluid Dynamic Turbulent Separated Flows And Transonic Potential Flows" Ph. D , Thesis, Mechanical Department, Univ. of state, 1997.

**[6]**- Lars Davidson "High lift Airfoil Flow Simulation Using A Two – Layer Reynolds Stress Transport Model " International Symposium on refined flow and turbulence measurement, Paris, Sep. 7-10, 1992.

[7]Yoshinodai, S. ,Satoko, K. and Kandasurugadia, C. "Direct Simulation Of A Flow Around An Airfoil " Institute of Space and Astronautically Science, 2000.

[8]Dahlstrom, S. Davidsony, L. " Large Eddy Simulation OF The Flow Around Aerospatiale A-Aerofoil " European Congress on Computational Methods in Applied Sciences and Engineering, ECCOMAS 2000.

[9]Dahlstr¨om , S. and Davidson, L."Large Eddy Simulation Of The Flow Around An Airfoil " AIAA Aerospace Sciences Meeting and Exhibit 8–11 January 2001.

[10]Dahlstr¨om, S. and Davidson, L. "Large Eddy Simulation Applied To A High Reynolds Flow Around An Airfoil Close To Stall" J. AIAA Aerospace Sciences Meeting and Exhibit 6–9 January 2003.

[11]Soshi Kawai and Kozo Fujii" Prediction of a Thin-Airfoil Stall Phenomenon Using LES/RANS Hybrid Methodology with Compact Difference Scheme" J. AIAA Fluid Dynamics Conference and Exhibit, 2004.

[11]Rupesh B. Kotapati-Apparao, Kyle D. Squires "Prediction of the Flow over an Airfoil at Maximum Lift" MAE Department, Arizona State University, Aerospace Sciences Meeting, AIAA 2004

[12]Kurzin, V. B." Using The Perturbation Method To Solve The Problem OF Separated

[13]Eisenbach,S., Friedrich, R" Large-eddy simulation of flow separation on an airfoil at a high angle of attack and $Re = 10^5$ using Cartesian grid" Theory. Computational. Fluid Dynamic. 22: 213–225, 2008.

[14]Thompson J. F., Thomas F. C., and Mastin C. W., "Automatic Numerical Generation of Body Fitted Curvilinear Coordinate System For Field Containing Any Number of Arbitrary Two Dimensional Bodies", J. of computational Physics, Vol. 15, P. 299-319, 1974.

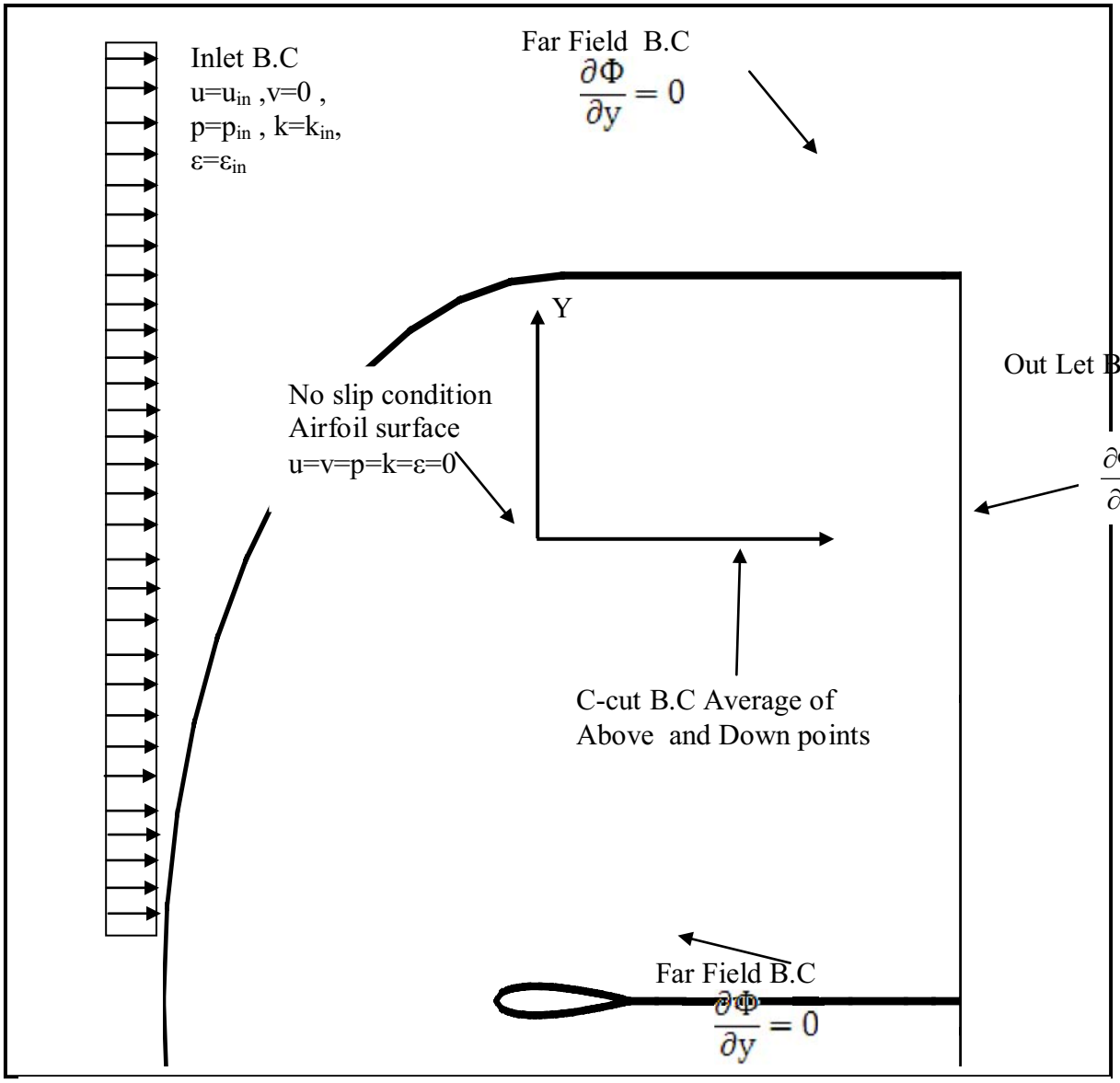


**Figure (1) Boundary Conditions of Present Study**

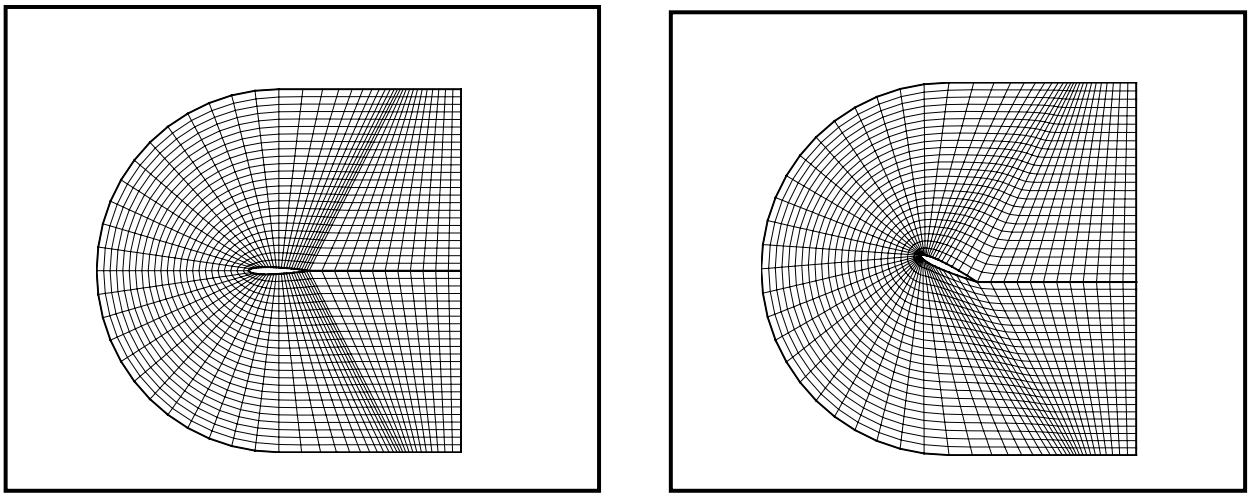

**Figure (2) Grid Generation**

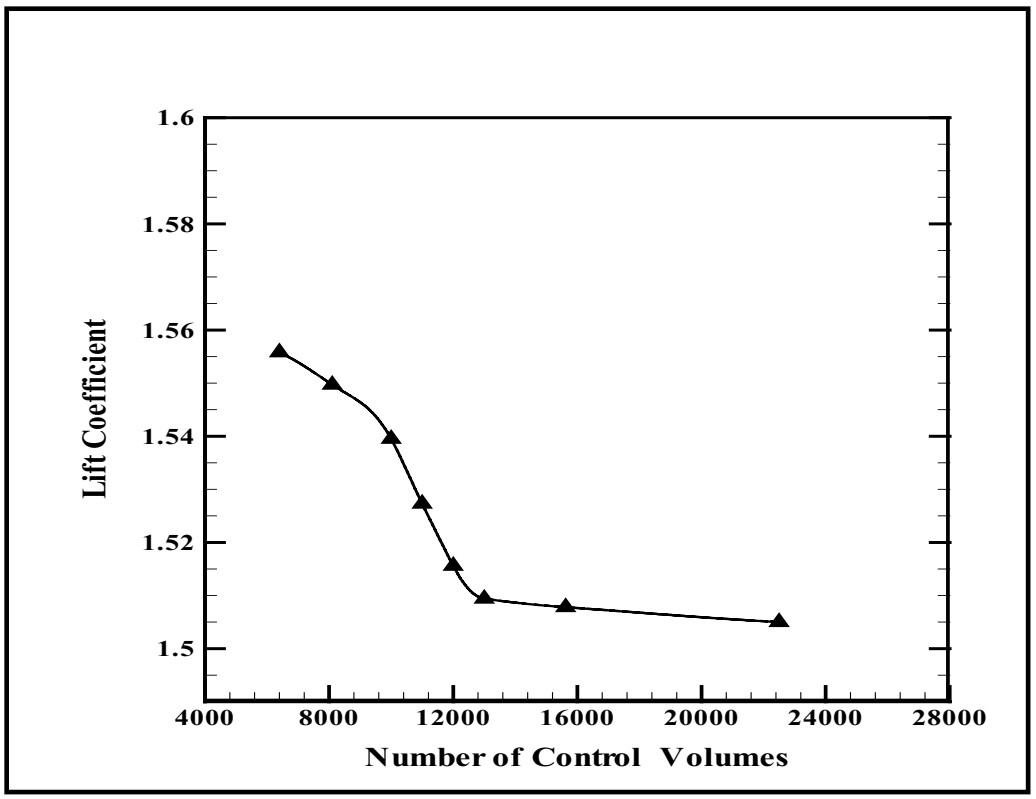


**Figure (2) Variation of Lift Coefficient For NACA 0012 As Function of Control Volume For Re=2.5 x$10^6$ ,And AOA=$15^0$**

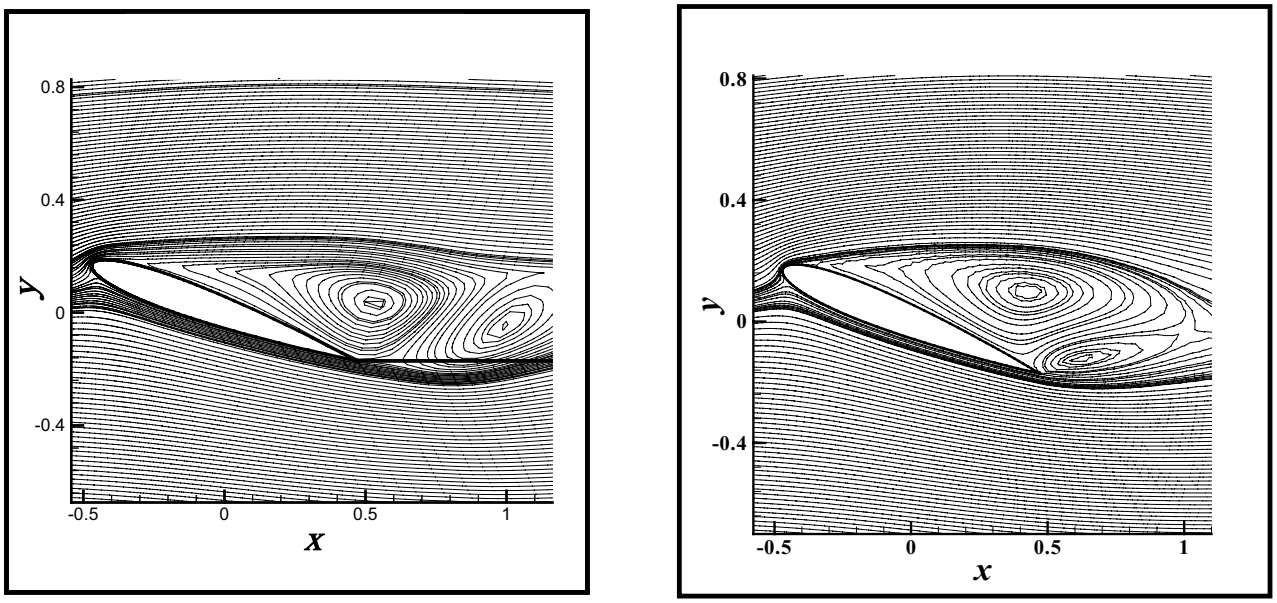


**Figure (4) Comparison of Stream Function Distributions Between The Present Work (Right) and The Computational study by [50] (Left) for NACA 0012 at Re=$10^6$ and Angle of Attack = 20°**

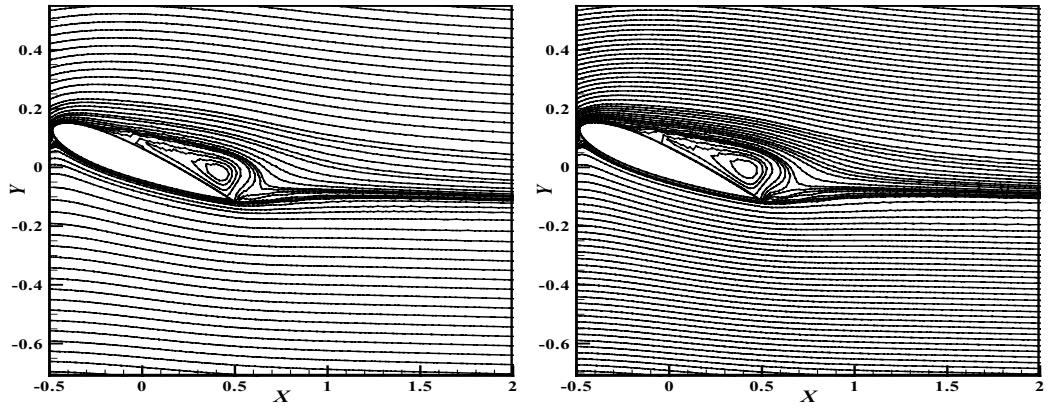


**Figure (2) Variation of**

(*b*) **Re=2.5x10$^6$ & AOA= 14°**

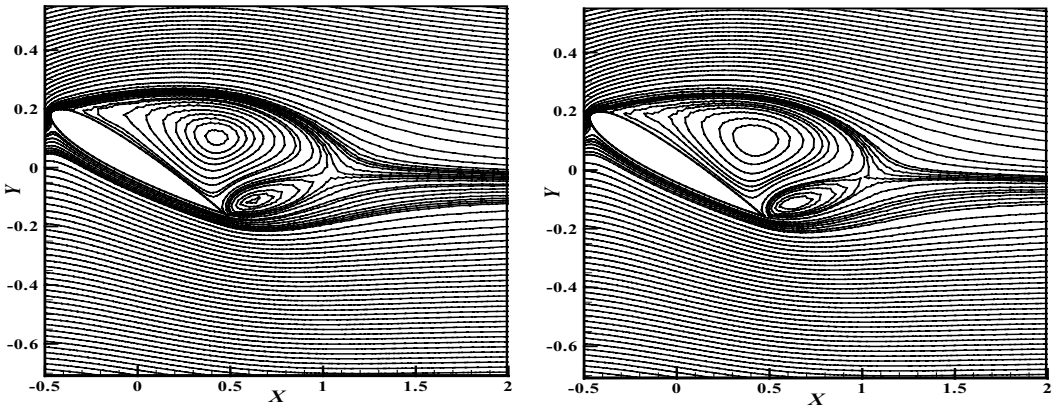


(*c*) **Re=1.5x10$^6$ & AOA= 20°**

(*d*) **Re=2.5x10$^6$ & AOA= 20°**

**Figure(5) Different Streamlines Distribution Over a NACA 0012 Airfoil at Re=1.5x10$^6$ & Re=2.5x10$^6$ and Angles of Attack (AOA) =14° & 20°**

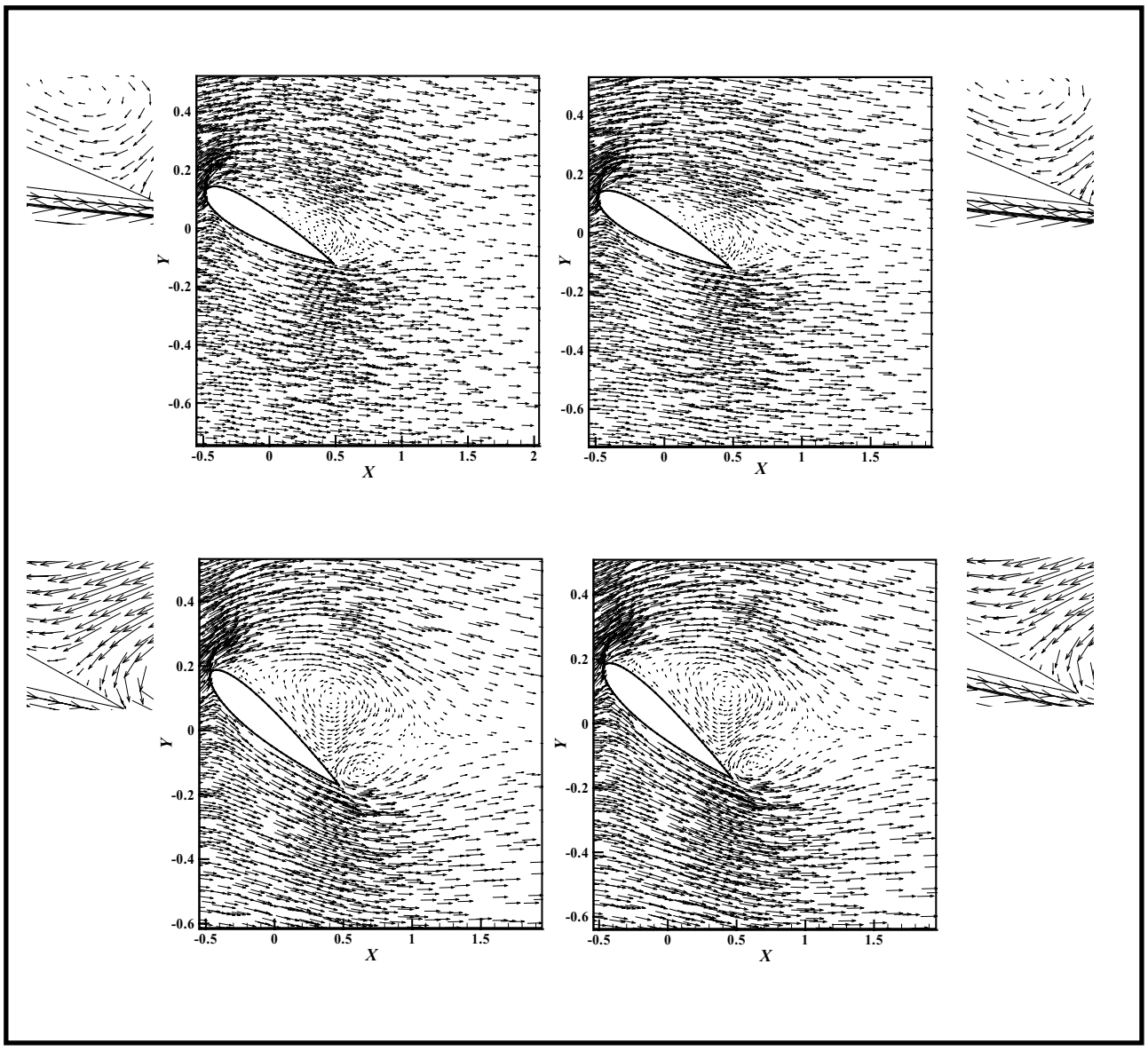


**Figure(6) Different Velocity Vector Field Results Over a NACA 0012 Airfoil at Re=1.5x10$^6$ & Re=2.5x10$^6$ and Angles of Attack (AOA) =14° & 20°**

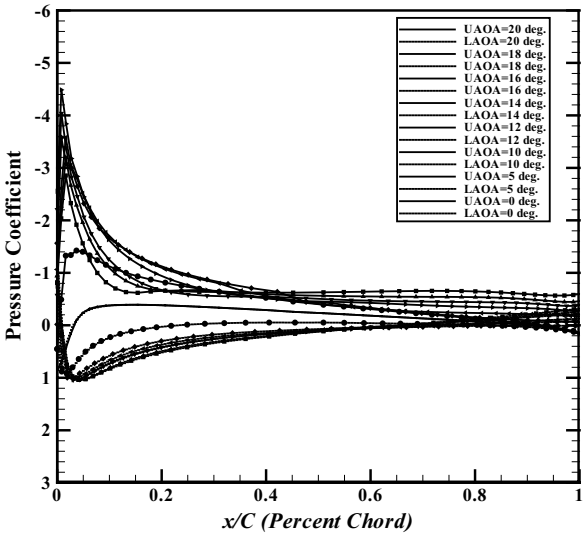


**Fig.(7) Effect The Variation of Angle of Attack On Pressure Coefficient($C_p$) Distribution Over a NACA 0012 Airfoil For Re=$10^6$**

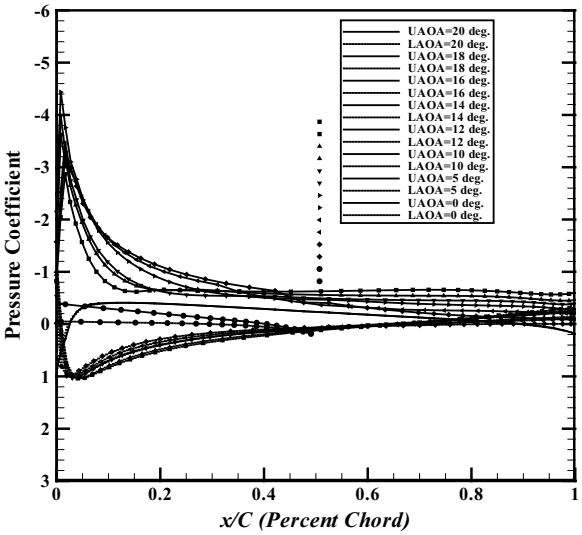


**Fig.(8) Effect The Variation of Angle of Attack On Pressure Coefficient ($C_p$) Distribution Over a NACA 0012 Airfoil For Re=1.5x$10^6$**

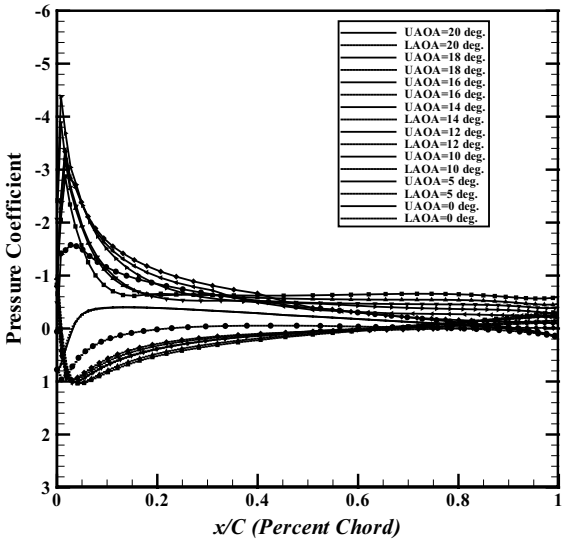


**Figure(9) Effect The Variation of Angle of Attack On Pressure Coefficient ($C_p$) Distribution Over a NACA 0012 Airfoil For Re=2x$10^6$**

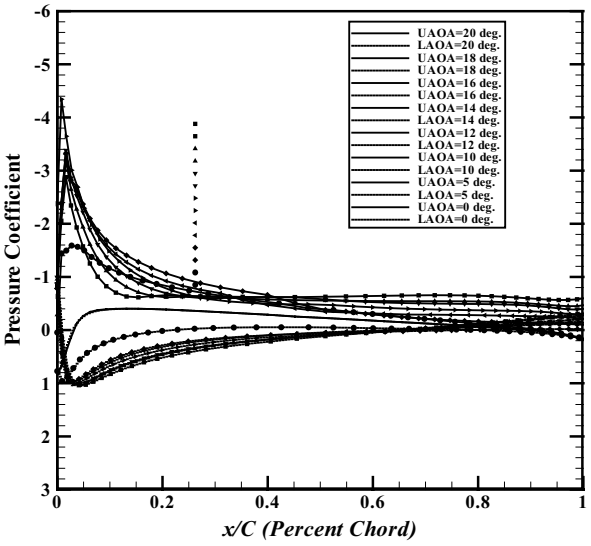


**Fig.(10) Effect The Variation of Angle of Attack On Pressure Coefficient ($C_p$) Distribution Over a NACA 0012 Airfoil For Re=2.5x$10^6$**

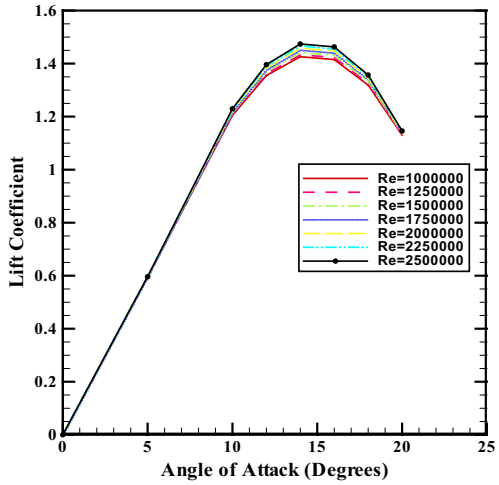


**Fig.(11) Effect The Variation of Turbulent Reynolds Numbers on The Lift Coefficient With Different Angle of Attacks For NACA0012**

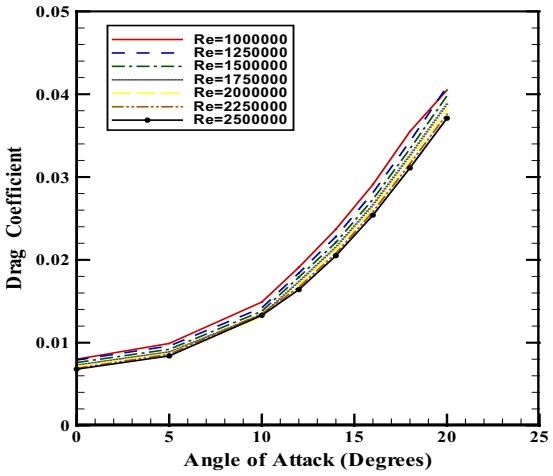


**Fig.(12)Effect The Variation of Turbulent Reynolds Numbers on The Drag Coefficient With Different Angle of Attacks For NACA 0012**

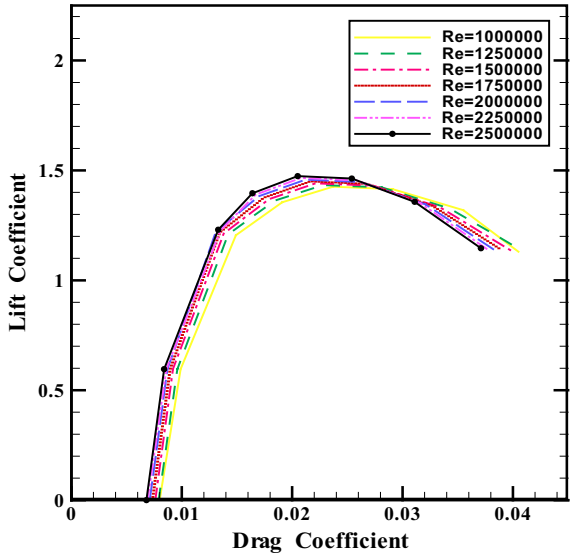


**Figure(13)Lift Versus Drag Coefficient Curve of The NACA 0012 Airfoil For Different Turbulent Reynolds Numbers**